RADIATED EMISSIONS FROM COMMON-MODE CURRENTS

by

Clayton R. Paul
Dept. of Electrical Engineering
University of Kentucky
Lexington, KY 40506

and

Donald R. Bush
Information Products Division
International Business Machines Corp.
Lexington, KY 40511

Abstract

Common-mode currents on interconnect cables and cables within a product are significant contributors to the overall radiated emissions of that product. This paper describes an experiment which shows that: (1) levels of common-mode currents are difficult to predict but (2) accurate predictions of their radiated emissions can be obtained if one measures these currents with a current probe. The experiment also illustrates the effectiveness of common-mode chokes (toroids) on the reduction of those currents and their related emissions.

I. Introduction

Consider a pair of wires carrying currents I_1 and I_2 as shown in Fig. 1(a). These currents can be decomposed into two auxiliary sets of currents. The first set is denoted as I_D and is referred to as differential-mode current. The differential-mode currents in the two wires at the same cross-sectional position are equal in magnitude and phase but oppositely directed. Equivalently we might say that the currents in the wires that are directed to the right have equal magnitudes but are 180^o out of phase. These types of currents constitute the normal or functional signals carried by the wires. The second set is denoted as I_C and is referred to as common-mode current. The common-mode currents in the two wires that are at the same cross-sectional position and directed to the right are equal in magnitude and phase.

In a functional design of a product, only the differential-mode currents are considered and their levels are easy to predict. Kirchhoff's current law applies to these currents. The common-mode currents are not easy to predict, and, if we amend Kirchhoff's current law to include displacement current, it will similarly apply. The "return path" for these common-mode currents is via displacement current and hence such factors as proximity of the wires to large metal objects become important.

Given the two currents I_1 and I_2 (perhaps individually measured with a current probe) it is a simple matter to decompose them into their common- and differential-mode currents. Write

$$I_1 = I_C + I_D \tag{1a}$$

$$I_2 = I_C - I_D \tag{1b}$$

Adding and subtracting these give

$$I_C = \frac{I_1 + I_2}{2} \tag{2a}$$

$$I_D = \frac{I_1 - I_2}{2} \tag{2b}$$

Any phase difference between I_1 and I_2 should be included. A current probe placed around both wires would give $2I_C$.

Common-mode currents of considerably less magnitude than differential-mode currents can produce the same level of radiated electric field as is illustrated in Fig. 1(b) and Fig. 1(c). The radiated emissions of the differential-mode currents subtract but do not exactly cancel since the two wires are not collocated. On the other hand, the emissions of the common-mode currents add.

A frequently-used model for predicting these emissions (given the currents) is based on the fields of the simple Hertzian dipole or infinitesimal current element shown in Fig. 2 [1]. The Hertzian dipole is an extreme simplification. The assumptions are:

(1) the length of the dipole, l, is infinitesimally small, and
(2) the dipole carries a phasor current I that is assumed to be the same (magnitude and phase) at all points along the dipole.

Assumption (2) means that the current does not go to zero at the endpoints which is impossible. Nevertheless, this Hertzian dipole can be used to give a reasonable model of other wire-type structures if used with care. The radiated electric field is given by [1]

$$E_r = 2\frac{Il}{4\pi}\,\eta_o\beta_o^2\cos\theta\left(\frac{1}{\beta_o^2 r^2} - j\frac{1}{\beta_o^3 r^3}\right) e^{-j\beta_o r} \tag{3a}$$

$$E_\theta = \frac{Il}{4\pi}\,\eta_o\beta_o^2\sin\theta\left(j\frac{1}{\beta_o r} + \frac{1}{\beta_o^2 r^2} - j\frac{1}{\beta_o^3 r^3}\right) e^{-j\beta_o r} \tag{3b}$$

$$E_\phi = 0 \tag{3c}$$

where the intrinsic impedance of free space is given by

$$\eta_o = \sqrt{\frac{\mu_o}{\epsilon_o}} = 120\pi \tag{4}$$

CH2487-7/87/000-0197 $01.00 © 1987 IEEE

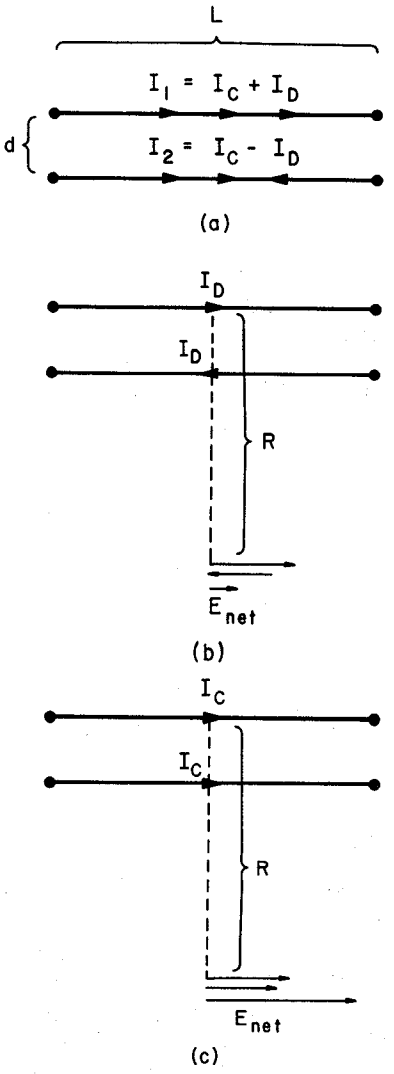

Fig. 1. Common-mode, I_C, and differential-mode, I_D, currents.

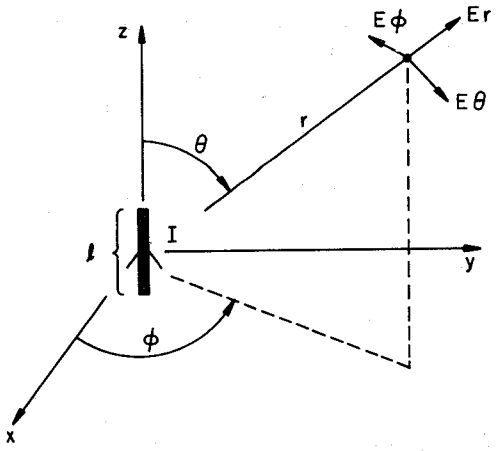

Fig. 2. The Hertzian dipole.

$$\doteq 377\ \Omega$$

and $\mu_o = 4\pi \times 10^{-7}$ H/m, $\epsilon_o \doteq 1/36\pi \times 10^{-9}$ F/m. The phase constant β_o is

$$\begin{aligned}\beta_o &= \omega\sqrt{\mu_o\epsilon_o} \\ &= \omega/u_o \\ &= 2\pi f/u_o \\ &= 2\pi/\lambda_o \quad \text{rad/m}\end{aligned} \tag{5}$$

where

$$u_o = \frac{1}{\sqrt{\mu_o\epsilon_o}} \tag{6}$$

$$\doteq 3 \times 10^8 \quad \text{m/s}$$

is the velocity of light in free space and

$$\lambda_o = \frac{u_o}{f} \tag{7}$$

is a wavelength at frequency f.

Generally only the 1/r far field term is retained so that

$$\begin{aligned}\vec{E}_{\text{farfield}} &= j\frac{Il}{4\pi}\,\eta_o\beta_o^2 \sin\theta\,\frac{1}{\beta_o r}\,e^{-j\beta_o r}\,\vec{a}_\theta \\ &= j\,\frac{60\pi Il f}{u_o r}\,e^{-j2\pi r/\lambda_o}\,\vec{a}_\theta \\ &\qquad\qquad r > \lambda_o/2\pi\end{aligned} \tag{8}$$

and $\vec{a}_\theta$ is a unit vector in the θ direction. The $1/r^2$ and $1/r^3$ terms are less than the 1/r term for distances greater than $r = \lambda_o/2\pi$ or roughly 1/6 of a wavelength. This far-field, near-field distance is cited at numerous places throughout the literature whether the structure being investigated conforms to the assumptions of the Herzian dipole or not. (Generally it doesn't.) Nevertheless, the Hertzian dipole, and particularly the far-field result given in (8), can be used to give reasonably accurate models of wire structures so long as the wire lengths are sufficiently short, **electrically**.

For example, consider the two wires in Fig. 1. Suppose the line length is L, the wire separation is d and point at which the total field is measured is R from the first wire. Also assume that this measurement point is in the plane of the two wires so as to give the maximum field (sin $\theta = 1$). If the wires are electrically short, $L << \lambda_o$, then we may approximate each structure as two Hertzian dipoles. Combining the fields given in (8) gives, for differential-mode currents,

$$\begin{aligned}E_{D_{max}} &= -j\frac{60\pi I_D L f}{u_o R}\,e^{-j\frac{2\pi R}{\lambda_o}} + j\frac{60\pi I_D L f}{u_o(R-d)}\,e^{-j\frac{2\pi(R-d)}{\lambda_o}} \\ &\doteq -j\frac{60\pi I_D L f}{u_o R}\,e^{-j\frac{2\pi}{\lambda_o}R}\left[1 - e^{j\frac{2\pi d}{\lambda_o}}\right] \\ &= -j\frac{60\pi I_D L f}{u_o R}\,e^{-j\frac{2\pi R}{\lambda_o}}\,e^{j\frac{\pi d}{\lambda_o}}\left[e^{-j\frac{\pi d}{\lambda_o}} - e^{j\frac{\pi d}{\lambda_o}}\right] \\ &= \frac{-120\pi I_D L f}{u_o R}\sin\left(\frac{\pi d}{\lambda_o}\right)e^{-j\frac{2\pi R}{\lambda_o}}\,e^{j\frac{\pi d}{\lambda_o}}\end{aligned} \tag{9}$$

where we have assumed R-d $\doteq$ R in the denominator of the second term. Taking the magnitude of this and assuming that the wires are electrically close together so that

$$\sin\left(\frac{\pi d}{\lambda_o}\right) \doteq \frac{\pi d}{\lambda_o}$$

gives

$$| E_{D_{max}} | \doteq \frac{120\pi I_D L f}{u_o R} \frac{\pi d}{\lambda_o} \qquad (10)$$

Substituting $\lambda_o = u_o/f$ gives

$$| E_{D_{max}} | \doteq \frac{120\pi^2}{u_o^2} \frac{I_D L d f^2}{R} \qquad (11)$$

$$= 1.316 \times 10^{-14} \frac{I_D f^2 L d}{R} \quad V/m$$

Similarly for the case of common-mode currents shown in Fig. 1(c)

$$E_{C_{max}} = -j\frac{60\pi I_C L f}{u_o R} e^{-j\frac{2\pi R}{\lambda_o}} - j\frac{60\pi I_C L f}{u_o (R-d)} e^{-j\frac{2\pi(R-d)}{\lambda}} \qquad (12)$$

$$\doteq -j\frac{60\pi I_C L f}{u_o R} e^{-j\frac{2\pi R}{\lambda_o}} e^{j\frac{\pi d}{\lambda_o}} \left[e^{-j\frac{\pi d}{\lambda_o}} + e^{j\frac{\pi d}{\lambda_o}}\right]$$

$$= -j\frac{120\pi I_C L f}{u_o R} \cos\left(\frac{\pi d}{\lambda_o}\right) e^{-j\frac{2\pi R}{\lambda_o}} e^{j\frac{\pi d}{\lambda_o}}$$

Again we assume R-d $\doteq$ R in the denominator of the second term. Once again taking the magnitude and assuming the wires are electrically close together so that

$$\cos\left(\frac{\pi d}{\lambda_o}\right) \doteq 1$$

gives

$$| E_{C_{max}} | \doteq \frac{120\pi I_C L f}{u_o R} \qquad (13)$$

$$= 1.257 \times 10^{-6} \frac{I_C L f}{R} \quad V/m$$

Note that the emissions for differential-mode currents given in (11) vary as the "loop area", Ld, and as the square of the frequency. The common-mode current emissions given in (13) depend only on the line length L and vary directly with frequency. We will use the simple common-mode model given in (13) to provide predictions where the common-mode current is measured with a current probe. In this case the current probe will measure $2I_C$ so that in terms of the current probe reading, $I_{cur\ probe}$, (13) becomes

$$| E_{C_{max}} | = 6.28 \times 10^{-7} \frac{I_{cur\ probe}\, L f}{R} \quad V/m \qquad (14)$$

This result is equivalent to replacing the wires with a single wire bearing $I_{cur\ probe}$ and using (8) directly.

The objectives of this paper are two-fold. It is intended to first show that common-mode currents on cables can be a significant contributor to radiated emissions and these currents are not at all simple to predict. Secondly, it is intended to show that accurate predictions of the radiated emissions from common-mode currents can be obtained using (14) *if* the common-mode currents are measured with a current probe. The lethality of common-mode currents can be easily demonstrated. The FCC Class B radiated emission limit at 30 MHz is 40 dB μV/m or 100 μV/m. Substituting this and a measurement distance of R = 3m into (13) shows that for a L = 1 meter length of cable, a common-mode current of $I_C = 8\mu A$ will meet the FCC Class B limit! Any additional common-mode current will exceed the Class B limit! The simple experiment we will show clearly demonstrates that it is a simple matter to generate common-mode currents on cables, and those radiated emissions can easily exceed the FCC Class B limit by a considerable amount. In the experiment to be shown, a battery was used to power all modules so that there was no connection to the commercial power system (frequently thought to be the prime contributor to common-mode currents). Yet this device that was battery powered exceeded the FCC Class B limit by as much as 25 dB!

II. The Experiment

A simple device shown in Fig. 3 was constructed. A 10 MHz square wave oscillator drove one gate of a 74LS04 hex inverter. The output of the inverter was connected via a 1 meter length of ribbon cable to the input of a similar 74LS04 hex inverter. The ribbon cable consisted of three wires each of which was #28 gauge (7x32) separated by 50 mils. One outside wire carried +5V to the far inverter while the other outside wire was the common. The middle wire carried the output signal of the near inverter. A 9-volt battery and a 7805 regulator provided the 5V supply. A photograph of the device is shown in Fig. 4. A copy of the board land configurations (solder side) is shown in Fig. 5.

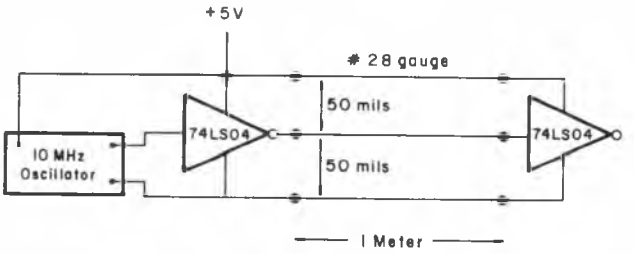

Fig. 3. Schematic of the device tested.

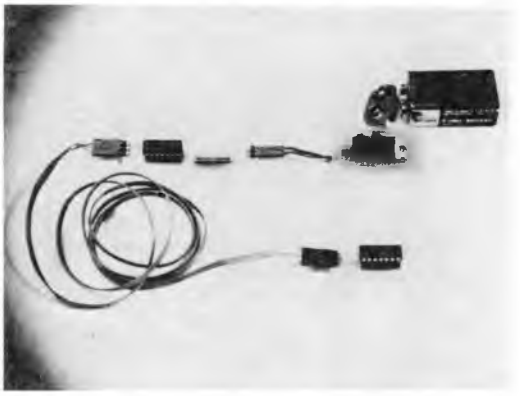

Fig. 4. Photograph of the device tested.

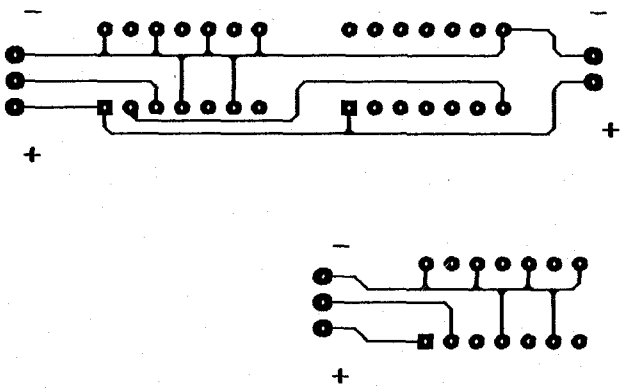

Fig. 5. Layout of printed circuit boards for the device.

The radiated emissions were measured in the semi-anechoic chamber at the IBM Information Products Division EMC Lab in Lexington, Kentucky. This facility is regularly used for EMC developmental testing and its accuracy has been verified by comparison to numerous other facilities. The measured data to be shown were obtained over the frequency range of 30 MHz to 200 MHz using a biconical antenna. The antenna and the test cable were positioned parallel to the chamber floor (horizontal) and both were 1 meter above the floor. The separation between them was 3 meters. So the antenna was oriented parallel to the cable in order to obtain the maximum emissions.

A correction for reflections from the ground plane should be applied to (14). Consider replacing the ground plane with the image of the cable common-mode current as shown in Fig. 6. Using (8) once again but adding the reflected wave gives

$$E_{C_{max}} = -j\,\frac{60\pi I_{cur\ probe} L\, f}{u_o R}\, e^{-j\frac{2\pi R}{\lambda_o}} \qquad (15)$$

$$+ j\,\frac{60\pi\, I_{cur\ probe} L\, f}{u_o \sqrt{R^2 + 4H^2}}\, e^{-j\frac{2\pi\sqrt{R^2+4H^2}}{\lambda_o}}$$

where H=1m denotes the height of the cable and the antenna above the ground plane and R=3m is the separation between the two. Simplifying (15) and taking the magnitude gives

$$\left| E_{C_{max}} \right| = \frac{60\pi I_{cur\ probe} L\, f}{u_o R}\, F \qquad (16)$$

where

$$F = \left| 1 - \frac{R}{\sqrt{R^2 + 4H^2}}\, e^{-j\frac{2\pi}{\lambda_o}\left[\sqrt{R^2+4H^2} - R\right]} \right| \qquad (17)$$

Thus to correct for ground plane reflections we multiply the previous result in (14) by F:

$$\left| E_{C_{max}} \right| = 6.28 \times 10^{-7}\, \frac{I_{cur\ probe} L\, f}{R}\, F \ \ V/m \qquad (18)$$

Table 1 shows values of this correction factor, F, for the test dimensions (R=3m, H=1m) for the frequencies of the test.

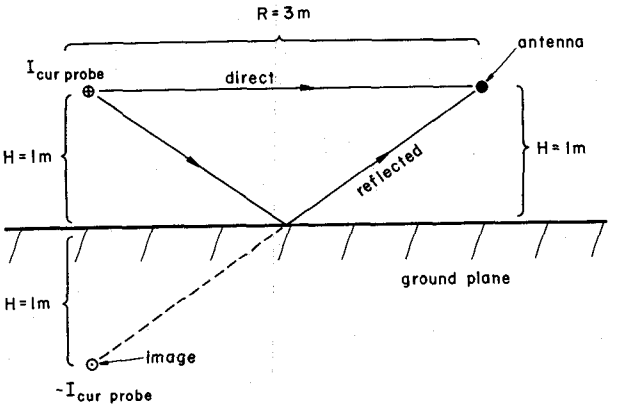

Fig. 6. Replacing the ground plane with the image of the cable common-mode current.

TABLE 1.

Ground Reflection Correction Factor F
(R = 3m, H = 1m)

frequency (MHz)	F	F(dB)
30	.384	-8.3
40	.488	-6.2
50	.593	-4.54
60	.698	-3.1
70	.801	-1.93
80	.902	-.9
90	1.000	0
100	1.094	.78
110	1.184	1.47
120	1.269	2.07
130	1.350	2.61
140	1.425	3.08
150	1.495	3.5
160	1.558	3.85
170	1.616	4.17
180	1.667	4.44
190	1.712	4.67
200	1.750	4.86

In the vicinity of 100 MHz, the ground reflection produces no significant effect, whereas at 30 MHz the correction is on the order of -8dB and at 200 MHz the correction is on the order of 5 dB.

A current probe was used to measure the common-mode current on the cable. The probe is manufactured by Fischer Custom Communications and is the F-33-1 model [2]. It has a transfer impedance of +15 dBΩ flat over the frequency range measured. The current probe is placed at the midpoint of the cable and the current measured. A photograph of the probe output measured on the spectrum analyzer is shown in Fig. 7 and these readings are denoted as V_{SA}. The probe transfer impedance must be subtracted from these readings to give the common-mode current:

$$I_{cur\ probe}\,(dB\mu A) = V_{SA}\,(dB\mu V) - Z_T \qquad (19)$$
$$= V_{SA}(dB\mu V) - 15$$

A 40 foot length of RG - 55U coaxial cable connected the probe to the spectrum analyzer. The loss of of this cable was measured and must be added to the values in (19).

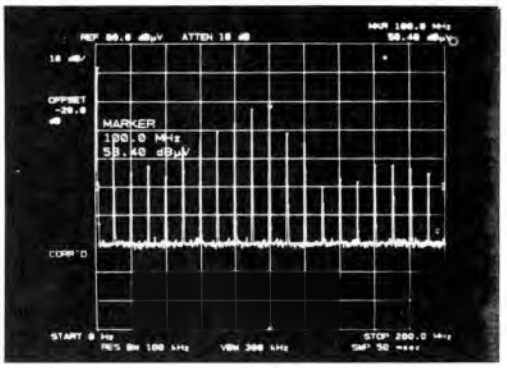

Fig. 7. Current probe output, V_{SA}, measured on spectrum analyzer.

In dB, the combination of (19), (18), (17) gives the predicted radiated emissions at each frequency as

$$E(dB\mu V/m) = -13.58 + V_{SA}(dB\mu V) - Z_T(dB) + \\ + 20\log_{10}(f_{MHz}) + F(dB) + \text{Cable Loss}(dB) \qquad (20)$$

III. The Results

The oscillator has a base frequency of 10 MHz so only harmonics of 10 MHz appear in the radiated emissions. A plot of the radiated emissions is shown in Fig. 8. The predicted values using (20) are shown on the plot denoted by X. The predictions are within 3dB of the measured data except at 50 MHz, 80 MHz, and 130 MHz.

The common-mode current was then measured at 5 cm intervals along the cable. Table 2 shows the levels at these measurement points for the 10th harmonic of 100 MHz.

TABLE 2.

$I_{cur\ probe}$ vs. Cable Position

f = 100 MHz

Position of current probe from oscillator end	$I_{cur\ probe}$ (dBμA)
5cm	38.7
10cm	40.7
15cm	41.9
20cm	42.6
25cm	43.4
30cm	44.3
35cm	44.7
40cm	45.1
45cm	44.7
50cm	44.4
55cm	43.9
60cm	43.2
65cm	41.9
70cm	41.1
75cm	40.2
80cm	39.5
85cm	38.4
90cm	35.5
95cm	.34.0

Note that even though the cable is $1/3\lambda_0$ at 100 MHz, the common-mode current does not display an extreme variation with position. So it appears that for these dimensions and this frequency range (a common case of interest) that using the measured common-mode current at the midpoint of the cable can produce reasonably accurate predictions of radiated emissions.

In order to confirm that the dominant radiated emissions are due to common-mode current and not differential-mode current, the 74LS04 load was removed and the radiated emissions remeasured. These results are shown in Fig. 9. Comparing Fig. 8 and Fig. 9, we see that the levels are generally the same. The common-mode current was measured for this configuration and the predictions are also shown on Fig. 9.

IV. Reduction of Common-Mode Current Emissions with Toroids

Ferrite cores (common-mode chokes or toroids) can be an effective way of blocking common-mode currents on cables. To illustrate this we wound 4 turns of the cable about a round toroid. The inner radius of the "doughnut" is 1.75 centimeters, and the toroid is made of #43 material [3].

The radiated emissions along with the predictions using the measured common-mode current at the midpoint of this cable are shown in Fig. 10. Comparing Fig. 8 and Fig. 10, we see that the toroid has reduced the radiated emissions by over 20 dB at some frequencies. Note also that, once again, accurate predictions of the radiated emissions can be obtained using (20) and the measured common-mode current.

V. Conclusions

This paper has shown that common-mode currents on cables can be a significant (often primary) contributor to radiated emissions of those cables. Simply eliminating the hardware connection to the commercial power system will not eliminate those common-mode currents as has been suggested [4]. The test circuit was battery powered yet significant common-mode currents were generated.

It was also shown that reasonably accurate predictions of the radiated emissions of those common-mode currents can be made if one measures the common-mode currents with a current probe. This technique can be effectively used as a diagnostic tool. It has been the authors' experience that radiation from common-mode currents on cables dominate the cable's differential-mode current radiation in the frequency range of 30 MHz to 200 MHz. A preliminary test of a product's radiated emission profile can be made in a semianechoic chamber and a current probe can be used to diagnose which cable is the primary contributor. (All cables except the AC power cord may be disconnected in order to confirm this.) Then modifications can be made in the design lab and the effect of those modifications can be confirmed **in the design lab** by using a portable spectrum analyzer and a current probe without tying up the EMC chamber. If the modification reduces the cable's common-mode current at the problem frequency then there is confidence that the radiated emissions from that current will be similarly reduced and scheduling the EMC chamber would be worthwhile. If the

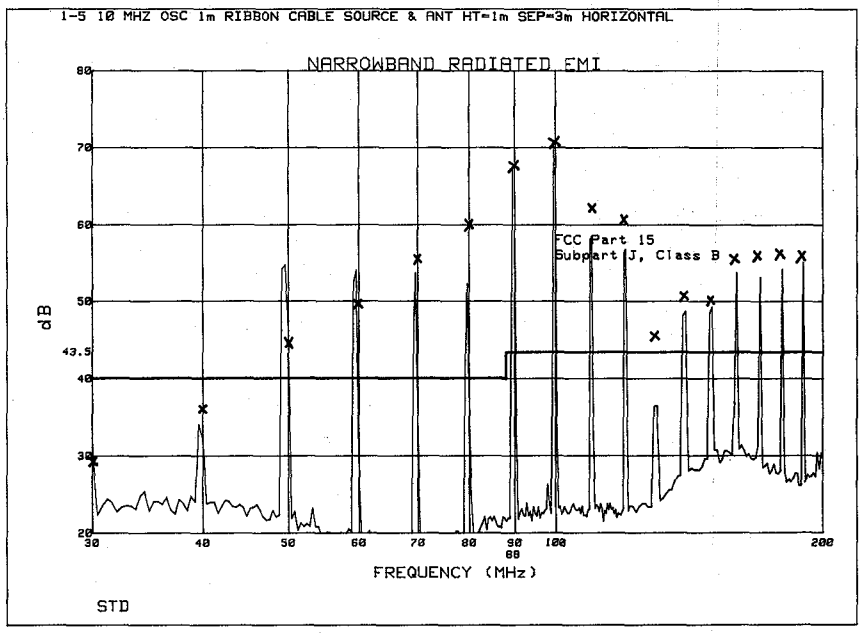

Fig. 8. Measured and predicted (x) radiated emissions of the device.

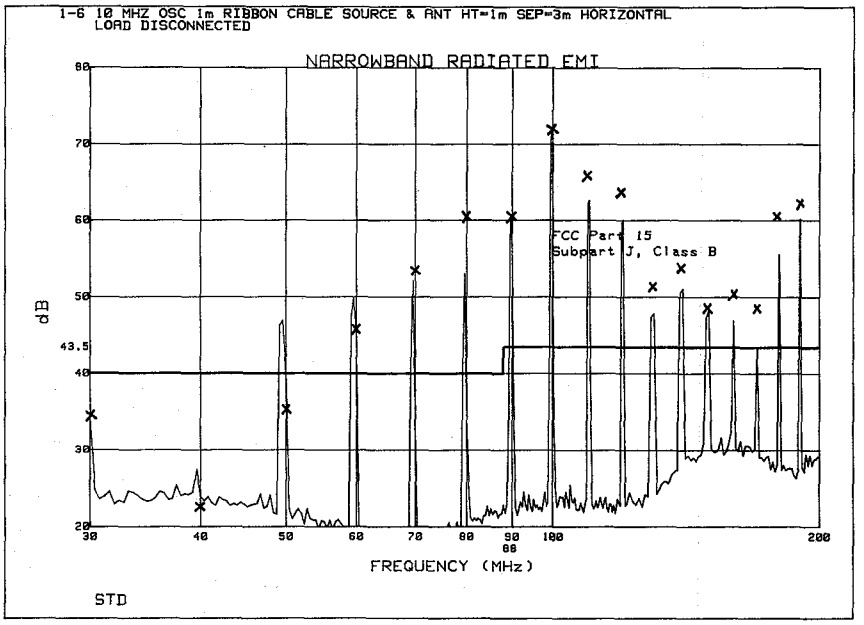

Fig. 9. Measured and predicted (x) radiated emissions of the device with the load removed.

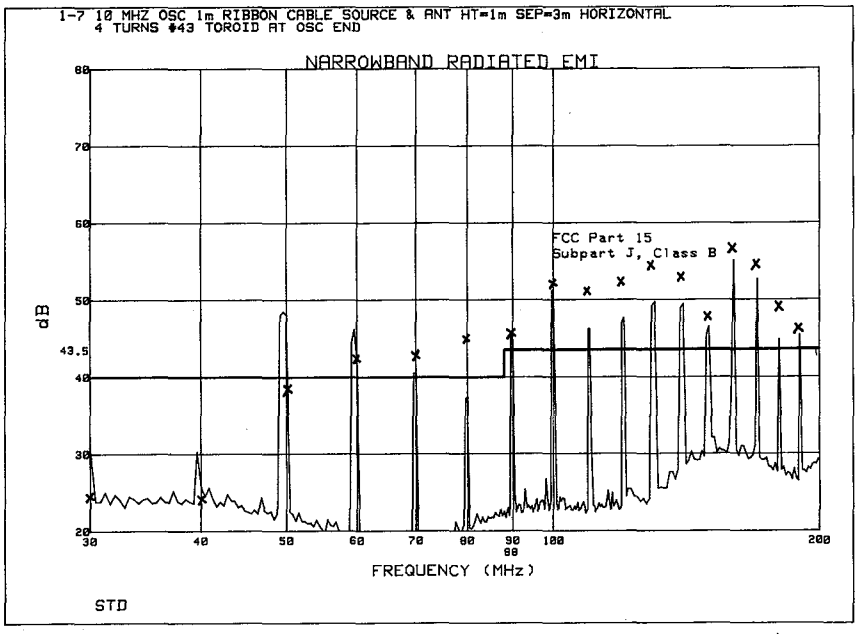

Fig. 9. Measured and predicted (x) radiated emissions of the device with the cable wrapped 4 turns through a #43 ferrite toroid.

modification did not reduce the common-mode currents of the cables (or even increased them) then scheduling the EMC chamber would probably be a waste of time.

And finally the effectiveness of common-mode chokes (toroids) in blocking common-mode currents on cables was demonstrated. Unlike shielded cables, toroids do not require a "quiet ground" (which generally doesn't exist) in order to effectively reduce emissions from common-mode currents on cables. The authors have experienced cases where shielding a cable can actually increase radiated emissions. In effect "grounding" the cable shield to a noisy ground point on the product has produced an efficient antenna (the cable shield). However, even with the use of the toroid, the radiated emissions from this simple device exceed the FCC Class B limit. So even if this simple device performed some useful function, it could not be marketed in the U.S.! This simple test rather dramatically illustrates that meeting the regulatory limits in today's digital circuits is not a simple task and could serve as a useful demonstration of that fact to others.

REFERENCES

[1] C. R. Paul and S. A. Nasar, **Introduction to Electromagnetic Fields**, 2nd ed., McGraw Hill, 1987, pp. 502-508.

[2] Fischer Custom Communications, Box 581, Manhattan Beach, CA 90266, (213) 545-4617.

[3] Amidon Assocs., 12033 Otsego St., North Hollywood, CA 91607.

[4] R. K. Keenan, **Digital Design for Interference Specifications,** The Keenan Corporation, 1983.